

Title: Diagnosis tools for PEMFC using humidification interruption tests

Article Type: Full Length Article

Keywords: PEMFC; diagnosis; experimental characterisation; water distribution; performance indicators

Corresponding Author: Dr. Jordi Riera, Ph.D.

Corresponding Author's Institution: CSIC/UPC

First Author: Mauricio Primucci, Ph.D.

Order of Authors: Mauricio Primucci, Ph.D.; Maria Serra, Ph.D.; Jordi Riera, Ph.D.

Manuscript Region of Origin: SPAIN

Abstract: This article presents different diagnosis tools for Proton Exchange Membrane Fuel Cells based on the analysis of their dynamic evolution when the humidification of the inlet gases is interrupted. The diagnosis is aimed to know the internal state of the fuel cell with respect to the water distribution. The proposed diagnosis procedures combine the information of the time response with that extracted from Electrochemical Impedance Spectroscopy and consist in monitoring the evolution of a set of performance indicators during the humidification interruption. The article presents a study for the selection of these performance indicators, which are related to the physical phenomena inside the PEMFC, and describes the patterns that correspond to proper or improper water distribution.

1. INTRODUCTION

Among the different fuel cell technologies, Proton Exchange Membrane Fuel Cells (PEMFC) present some properties that make them the most appropriate for portable and transport applications: high efficiency, no emissions, solid electrolyte, low operating temperatures and high power density. However, one important issue of the PEMFC operation is the water management. The right water content is needed in the electrolyte, catalyst and diffusion layers to minimize the voltage losses. Different phenomena affect the water distribution inside the fuel cell. The generation of water by the reaction, the humidification of the inlet gases, the diffusion of water in the diffusion layers and the water transport through the membrane are the most important.

The procedure proposed in this work, aimed to diagnose the water distribution inside the PEMFC, is based on experimental characterisation techniques performed under special operating conditions and on models that allows the physical interpretation.

One important review of diagnosis tools applied to PEM fuel cells is the two-parts article by Wu et al. [2008a] and [2008b]. The article examines and discusses various electrochemical techniques and outlines for each one of the experimental procedures its capabilities and weaknesses. The experimental electrochemical techniques reviewed are the polarization curve, the current interruption, the Electrochemical Impedance Spectroscopy (EIS), the cyclic and CO stripping voltammetry and the linear sweep voltammetry. The pressure drop analysis is presented as a simple way to diagnose the formation of droplets in

the cell channels. Also more expensive techniques are explained as gas chromatography, neutron imaging and magnetic resonance imaging.

In this work only two of the diagnosis techniques described in the literature are used: the Polarisation Curve and the EIS. The Polarization Curve is the representation of the fuel cell performance through the static current-voltage response (Wu et al. [1], Ju et al. [2] and Srinivasan et al. [3]). While it gives useful information of the overall performance under specific operating conditions, the Polarisation Curve fails to give information about the performance of individual components within the cell and thus, it fails to differentiate the internal mechanisms between them. For example, flooding and drying inside a fuel cell cannot be distinguished with a single Polarization Curve. On the other hand, the technique cannot be performed during normal operation.

The EIS is a powerful technique for fuel cell study. This dynamic method can provide more information than steady-state experiments. Specifically, it can provide diagnostic criteria for evaluating the PEMFC internal state, as explained in MacDonald et al. [4] and Barsoukov et al. [5]. The main advantage of EIS is its usefulness to resolve, in the frequency domain, the individual contributions of the various phenomena determining the overall PEM fuel cell power losses: ohmic, activation and reactants concentration. Such a separation provides useful information both for optimization of the fuel cell design and for the selection of the most appropriate operating conditions.

Some diagnosis techniques performed under special conditions are mentioned in the literature, two of them are directly related to this work. In the article of

Gebregergis et al. [6], flooding and drying faults are detected from the cell voltage and the impedance response of the cell. The flooding and drying processes are forced by the difference of the temperatures of the fuel cell and the gas inlet humidification, for both reactants, H_2/O_2 , during a long time (more than 120 minutes each process). The work presented by Fouquet et al. [7], treats the monitoring of the flooding and drying processes (varying the inlet gas relative humidity) using a model-based approach coupled with AC impedance measurements (EIS).

The objective of the work presented here is to describe easy, cheap, simple, low intrusive procedures and tools for the on line diagnosis of internal water distribution of PEM fuel cells.

The procedures presented in this work use the information extracted from the Humidification Interruption Test in order to study the water transport and accumulation. This test, described by Primucci et al. [8], is a dynamic characterisation technique that combines the time evolution analysis of certain measured stack variables with the time evolution analysis of the EIS characteristics, when the inlet gases humidification are completely interrupted in the PEMFC. Based on these analysis, some performance indicators are selected. The diagnosis will be achieved thanks to the monitorisation of these performance indicators.

The paper is distributed as follows: in section 2, the system and experimental set up are described and in sections 3 and 4, the experimental test results are showed. Section 5 presents an analysis of the results. In section 6, the different

performance indicators to be used as diagnosis tools and the diagnosis procedures are described. In section 7 a comparative analysis of the two diagnosis tools is performed and, finally, in section 8, the main conclusions of the work are summarised.

2. DESCRIPTION OF THE SYSTEM AND EXPERIMENTAL TEST

This work is based on the experimental results obtained using a single fuel cell with the following characteristics. Builder: Electrochem, Model: EFC05-01SP, Active Area: 5cm², Membrane Electrolyte Assembly: Nafion 115, 1mg. Pt/cm² (platinum load at both sides) and Toray carbon fiber paper "TGP-H-060" with 0.19mm thickness as GDL.

The experimental set-up allows the interruption of the humidification system on any side (cathode and/or anode) thanks to parallel connections of gases with two ways valves that perform the interruption and restoration of the humidification (see Fig. 1).

At the same time that the humidification interruption test occurs, "short duration" EIS are performed periodically in order to study the frequency response evolution during the humidification interruption and restoration.

The experiment has four different parts. In the first one, current load and full humidification of inlet gases conditions are fixed and, after that, some time is given to let the fuel cell achieve a stationary operating point. When attained, a EIS with points in the interval 0.1 - 10⁴ Hz is performed. The second part starts

when applying the by-pass of one of the inlet-gases humidifiers leading to the humidifier interruption phase. During this phase, important water transfers occur inside the fuel cell, which are noticed by recording some of the main measurable variables of the set-up and by performing periodic EIS. The duration of these EIS is a little shorter, $0.2-10^4$ Hz, to perform the EIS analysis during a same quasi static operating state. When the measurable variables of the fuel cell arrive to a new steady state, or their evolution tend to non reasonable operating values, the third part of the test is launched reconnecting the humidification eliminating the by-pass. During this third phase the fuel cell suffers again important water transfers, which are also recorded. Once the fuel cell arrives to a new stationary state, the test gets into the fourth phase and a long EIS is performed.

3. RESULTS OF THE CATHODE HUMIDIFICATION INTERRUPTION

The dynamic evolution of the main variables of the fuel cell during the cathode humidification interruption test can be seen in Fig. 2, while Fig. 3 and Fig. 4 present the evolution of the EIS.

Observing the voltage in Fig. 2, a maximum can be seen during the cathode humidification interruption. The voltage increases during approximately three minutes and then, it has a maintained decrease until the humidification is restored. If Fig. 3 and Fig. 4 are observed, it is seen that, during this time interval, the Low Frequency Resistance (R_{LF}) has a decrease followed by an increase, and the High Frequency Resistance (R_{HF}) increases during all the

interruption time, but only slightly initially, and in a pronounced way about two minutes after the interruption.

When the humidification of the cathode inlet gas is restored, the cell voltage returns to its initial value without any peak. None of the analysed variables show maximums or minimums. About five minutes after the cathode humidification reconnection, the fuel cell has recovered the state it had before the humidification interruption, as can be seen in Fig. 2 and in Fig. 4. The fact that the system returns to its initial state is relevant and it makes possible to say that the diagnosis procedure is low intrusive, and therefore that the diagnostic is valid not only for the system before the test but also for the system after the test.

4. RESULTS OF THE ANODE HUMIDIFICATION INTERRUPTION

Anode humidification interruption tests were also performed. In Fig. 5 the dynamic evolution of the main variables of the fuel cell during the anode Humidification Interruption Test can be seen. Fig. 6 and 7 present the evolution of the EIS during humidification interruption and reconnection, respectively. However, in this case the different measured variables increase or decrease steadily, without presenting any peak. It can also be observed that the sensitivity of the system to the anode humidification interruption is much smaller than for the cathode case, in consequence, in the following only the cathode humidification interruption test will be treated.

5. ANALYSIS OF THE TEST RESULTS

The voltage behaviour is the result of different phenomena. The principal mechanisms affecting the cell voltage when the humidification of the inlet gases is changed are:

- a) **The oxygen partial pressure modification.** When the cathode humidification is interrupted, and thus the partial pressure of water vapour disappears, the oxygen partial pressure of the inlet gas increases what produces an increase of the cell voltage. Even if the water content in every cell layer into the cell was optimal, the humidification interruption would produce an increase of the voltage.
- b) **The diffusivity of gases modification.** When the humidification is interrupted, a drying action starts on all the cell components. In particular, the diffusion of gases in the diffusion layer depends on the water content in this layer. Because of that, if the system is over humidified, the oxygen diffusion will improve because the diffusion layer starts to dry. The Low Frequency Resistance (R_{LF}) decrease observed in Fig. 3 is due to the oxygen partial pressure increase and the improvement of the gas diffusion.
- c) **The membrane (and catalyst layer) water content modification.** At the same time that the water in the diffusion layer is being dried, the membrane also starts to dry, what is reflected through a slow increase of the High Frequency Resistance (R_{HF}). After approximately two minutes,

the membrane dries at a faster rate, because the water in the GDL and in the cathode catalyst layer has already moved out and is the membrane water content that starts to decrease. Hence, R_{HF} grows rapidly. Also, as a consequence of this lack of water inside the membrane, the reaction sites become more inaccessible to the protons and a reduction of the active area occurs.

With these different mechanisms affecting the cell voltage, it is clear that the cell voltage alone cannot be a good performance indicator for diagnosis of the water content distribution. We, then, require other specific performance indicators directly related to the water presence in the different parts of the cell.

During the time between the reconnection and the stabilisation, neither maximums nor minimums are observed. This is due to the fact that the different phenomena occur at the same time, what makes the data from this period less useful for diagnosis purposes. Something similar happens when the interruption is done in the anode humidification: the simultaneity of different internal phenomena makes this kind of tests less interesting as a discernment tool. Therefore, the diagnosis will be based on the analysis of the system evolution during the time that the cathode humidification is disconnected.

6. PERFORMANCE INDICATORS USED AS DIAGNOSIS TOOLS

Different performance indicators can be extracted from the experimental humidification interruption test. They are presented in the next sub-sections as the base of two different approaches for PEMFC diagnosis. The diagnosis of

the fuel cell can be applied in-situ, and gives information on whether the system humidification before the test was optimal or not. Since the tested system ends in the same state that it had before the test, the diagnosis corresponds to the tested system.

6.1. EIS relevant characteristics as performance indicators

The Relevant Characteristics of an EIS response contain very valuable information about the cell state. Figure 8 shows these characteristics as they are defined by Primucci et al. [9]. If the EIS Relevant Characteristics are properly monitored during the cathode humidification interruption, they can be useful to give a diagnostic of the fuel cell internal state. After a systematic analysis, three of them have been selected as performance indicators for the water distribution diagnosis: the low and high frequency resistances (R_{LF} and R_{HF}) and the frequency of the maximum phase ($f_{\phi_{max,LF}}$). R_{LF} can be interpreted as the concentration and activation resistance. Coming from a humidified state, if R_{LF} decreases, a diminution of the amount of water makes the oxygen transport easier in the GDL. If the drying process continues, a lack of water in the catalyst layer can be supposed and, in consequence, R_{LF} increases because of the loss of active sites. On the other hand, R_{HF} can be directly related with the membrane water content. Specifically, R_{HF} is inversely proportional to the membrane conductivity, which depends on the water content. Finally, $f_{\phi_{max,LF}}$ can be related with the diffusivity of the media. The easier the diffusion of gases through the media, the larger $f_{\phi_{max,LF}}$. Fig. 9 shows their evolution during a cathode humidification interruption, where the vertical lines mark the humidifier disconnection and reconnection times.

In Fig. 9 two zones of evolution can be distinguished. Zone 1 is characterized by an R_{LF} decrease, a slight increase in R_{HF} and a $f_{\phi_{max,LF}}$ increase. All these variations indicate an improvement of the water content distribution among the different components of the cell due to the drying action. In Zone 2, the voltage falls, R_{LF} increases and R_{HF} grows at a higher rate than in Zone 1. In this second zone, due to the persistent drying effect, the water starts to move out from the membrane to the cathode channel (due to the water concentration difference). This movement affects the membrane resistance, directly related to its water content and also reduces the reaction sites for hydrogen protons connected by water paths to the membrane. The best water content distribution situation is then just at the end of Zone 1.

Table 1 summarizes the trends of the Relevant Characteristics for Zone 1 and Zone 2. When Zone 1 duration is minimal, the system is optimally humidified denoting that there is no liquid water in the GDL and the membrane is conveniently humidified. As a conclusion, the proper distribution of water inside the fuel cell can be determined through the localisation of the limit that separates Zone 1 and Zone 2 in the plot of the performance indicators evolution during a cathode humidification interruption.

6.2. Equivalent circuit parameters as performance indicators

A second approach for PEMFC diagnosis with respect to the water distribution is employing the Equivalent Circuit concept (Bautista [10]). A simple equivalent circuit used to represent the PEMFC response consists of a resistance R_m in series with a Warburg element. The Finite Length Warburg element employed

has the following transfer function: $W(s) = \frac{R_W \cdot \tanh((s \cdot T_W)^{P_W})}{(s \cdot T_W)^{P_W}}$, where s is the Laplace complex variable, R_W , T_W and P_W , are the resistance, time constant and power of the Warburg element. This equivalent circuit is sufficient if the fuel cell is fuelled with air. The equivalent circuit parameters are fine tuned using the Zview® software.

In this approach the parameters selected as performance indicators among the equivalent circuit parameters are the membrane resistance, R_m , and the time constant and resistance of the diffusion process T_W and R_W , Fig. 10 shows the evolution of these three parameters during the cathode humidification test. After the analysis of the evolution of these parameters a diagnosis procedure is also based on the delimitation of two “Zones”. “Zone 1” is the zone where R_W and T_W decrease and R_m has slow increase. The humidification of the fuel cell is optimal when “zone 1” is minimal (see Fig. 10). Table 2 summarizes the trends of the Equivalent Parameters chosen as performance indicators for Zone 1 and Zone 2.

7. DISCUSSION

The two diagnostic tools, the one based in the EIS relevant characteristics and the one based in the Equivalent circuit parameters as performance indicators, look very similar although they are based on differently deduced indicators. But the difference is only apparent, an approximation of the equivalent circuit parameters from the relevant characteristics and can be summarised as follows (Primucci et al. [9]):

$$\begin{aligned}
R_m &\approx R_{HF} \\
R_W &\approx R_{LF} - R_{HF} \\
T_W &\approx \frac{1}{2\pi f_{\phi_{\max} LF}} \\
P_W &\approx -\frac{4}{\pi} \arctan \left(-\frac{2 \operatorname{Im}_{\operatorname{Im} ax LF}}{R_W} \right)
\end{aligned} \tag{1}$$

Then, there is an almost direct correspondence between the two sets of indicators, although they were deduced in a different way, and then the two diagnosis tools give similar results.

8. CONCLUSIONS

The Humidification Interruption Test technique is employed to obtain, from a PEMFC, a combination of time and frequency responses that give key information of the cell humidification state.

Two sets of performance indicators are identified to be used as diagnosis tools for the cathode humidification. These performance indicators are easy to obtain from the humidification interruption test and are related to physical phenomena present inside the fuel cell. The two diagnosis procedures, based on the monitorisation of the selected performance indicators during the test, prove to be equivalent, simple and effective.

Acknowledgments

The experimental tests were performed at the IRII (CSIC/UPC) laboratory. The authors acknowledge financial support from Spanish MICINN (DPI2010-15274 and DPI2011-25649). M.P. is grateful to the Generalitat de Catalunya (AGAUR Dept.) for the PhD Grant support.

References

- [1] J. Wu, X. Yuan, H. Wang, M. Blanco, J.J. Martin, J. Zhang, *Journal of Hydrogen Energy* 33, (2008) 1735-1746.
- [2] H. Ju, C.Y. Wang, *Journal of Electrochemical Society* 151, (2004) A1954-A1960.
- [3] S. Srinivasan, O.A. Velew, A. Parthasarathy, D.J. Manko and A.J. Appleby, *Journal of Power Sources* 36, (1991) 299-305.
- [4] D.D. Macdonald, *Electrochimica Acta* 51, (2006) 1376–1388.
- [5] E. Barsoukov, and J.R. Macdonald. *Impedance Spectroscopy: Theory, Experiment and Applications*, 2nd edition, (2005) Wiley & Son.
- [6] Gebregergis, A., Pillay, P., & Rengaswamy, R. 2010. *IEEE Transactions on industry applications*, 46, 295–303.
- [7] N. Fouquet, C. Doulet, C. Noullant, G. Dauphin-Tanguy and B. Ould-Bouamama. *Journal of Electrochemical Society* 151 (2004) A1954-A1960.
- [8] M. Primucci; M. Serra and J. Riera, *proc. of CONAPICE 2008, Zaragoza* (2008) 231-234.
- [9] M. Primucci; M. Serra and J. Riera, *proc. of “HYCELTEC 2008”, Bilbao* (2008) 1-26.
- [10] M. Bautista, Y. Bultel, J.-P. Diard, S. Walkiewicz. In *14ème Forum sur les Impédances Electrochimiques*, 221–230 (2002).

Table 1. Trends of the Relevant Characteristics for Zone 1 and Zone 2

Zone	$\Delta R_{LF} [\Omega]$	$\Delta f_{\phi_{max}} [Hz]$	$\Delta R_{HF} [\Omega]$
1	$< 0, \downarrow\downarrow$	$> 0, \uparrow$	$> 0, \uparrow$
2	$< 0 \rightarrow > 0, \uparrow\uparrow$	$> 0, \approx \text{cte}$	$> 0, \uparrow\uparrow$

Table 2. Trends of the Equivalent Parameters for Zone 1 and Zone 2

Zone	$\Delta R_w [\Omega]$	$T_w [s]$	$\Delta R_m [\Omega]$
1	$< 0, \downarrow\downarrow$	$< 0, \downarrow$	$> 0, \uparrow$
2	$< 0 \rightarrow > 0, \uparrow\uparrow$	$> 0, \approx \text{cte}$	$> 0, \uparrow\uparrow$

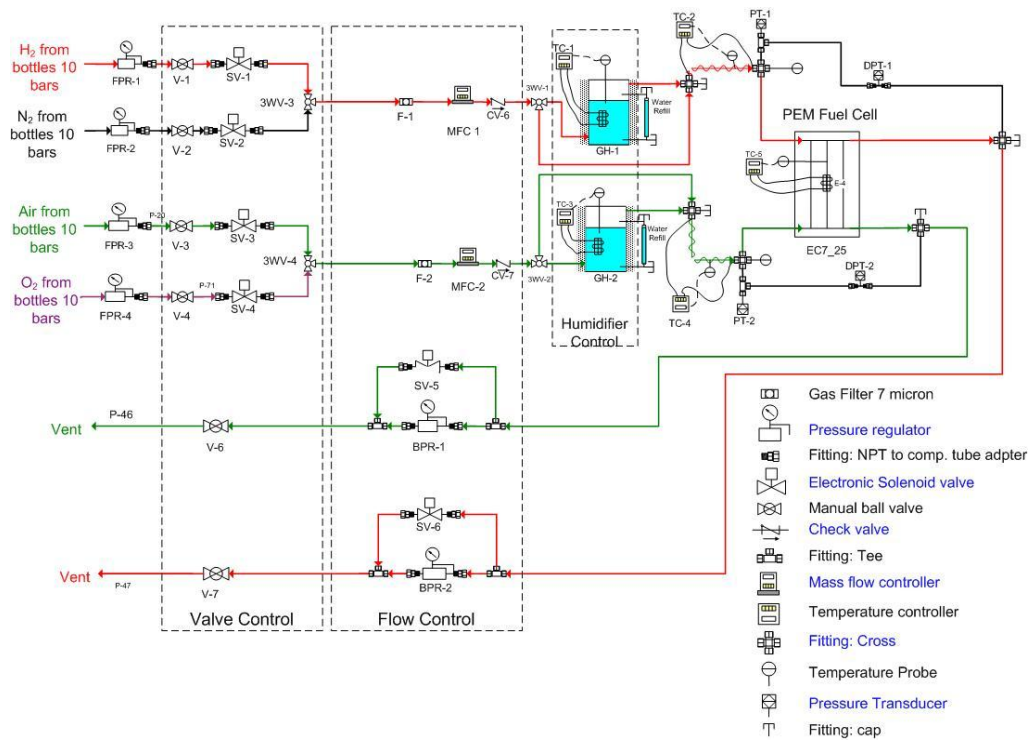


Fig. 1. Experimental setup for humidification interruption

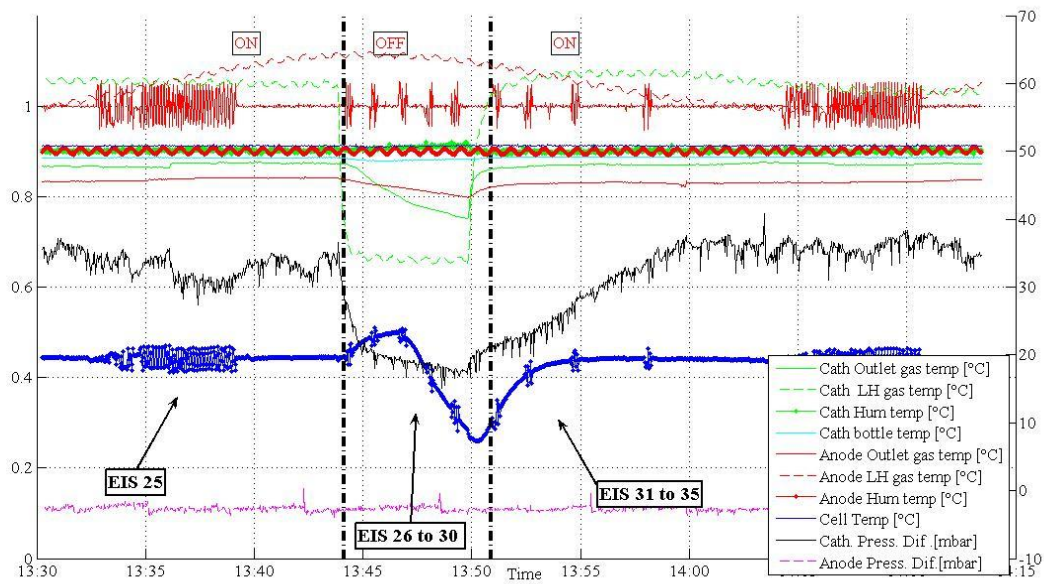


Fig. 2. Cathode humidification interruption test

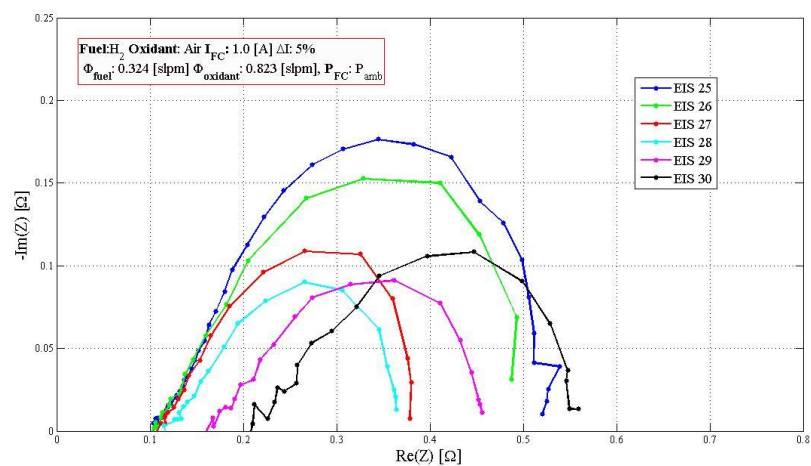


Fig. 3.EIS results during cathode humidification interruption

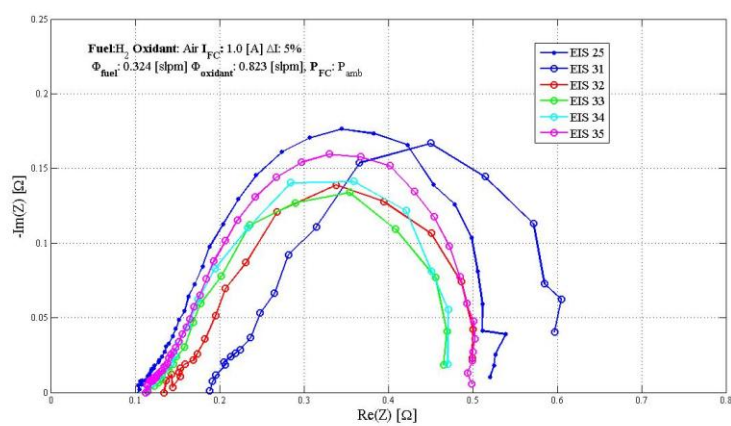


Fig. 4.EIS results after cathode humidification reconnection

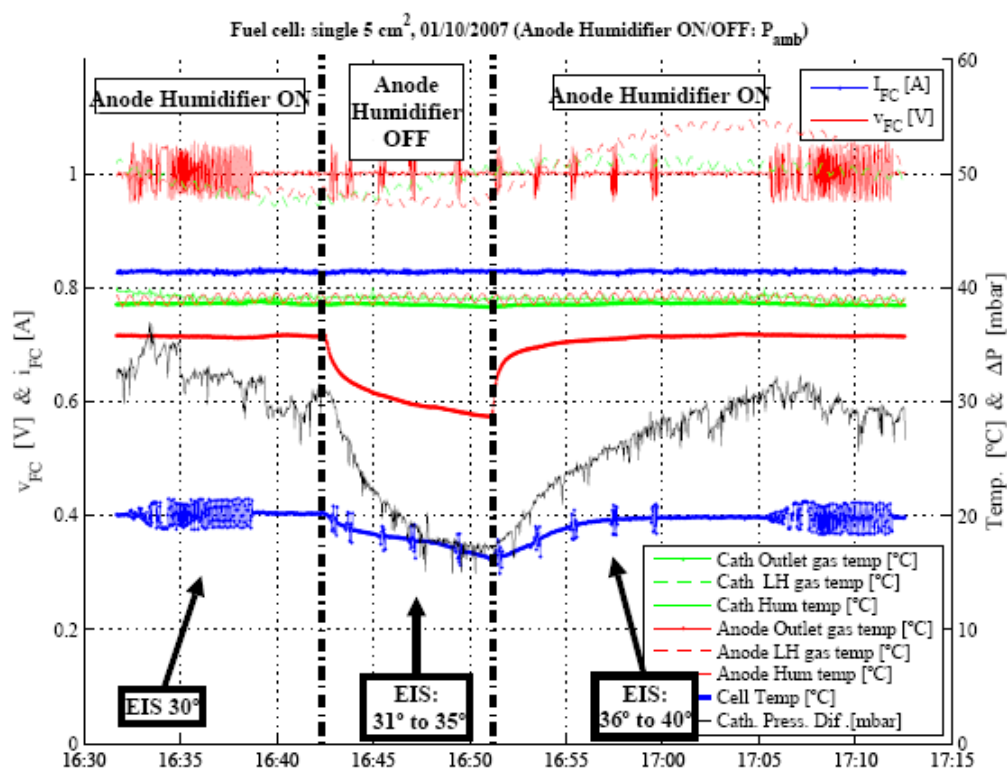


Fig. 5. Anode humidification interruption test

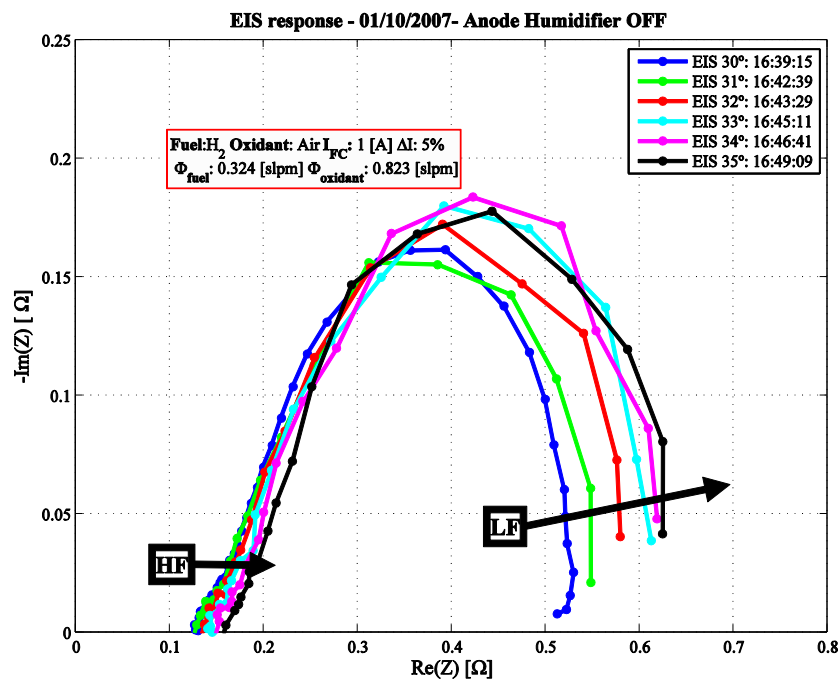


Fig. 6. EIS results during anode humidification interruption

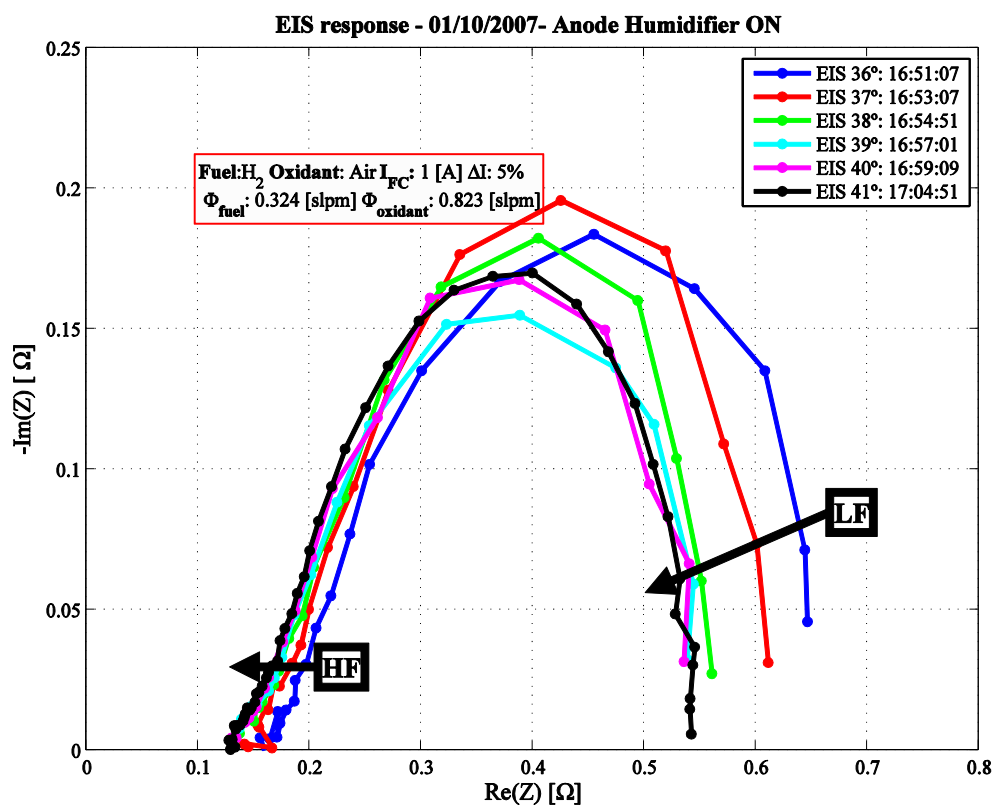


Fig. 7. EIS results after anode humidification reconnection

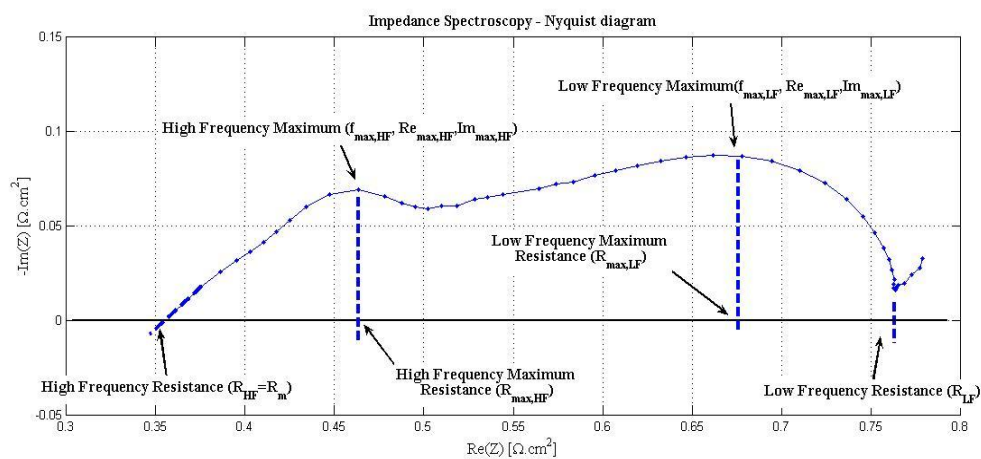


Fig. 8. EIS Relevant Characteristics a) Nyquist plot

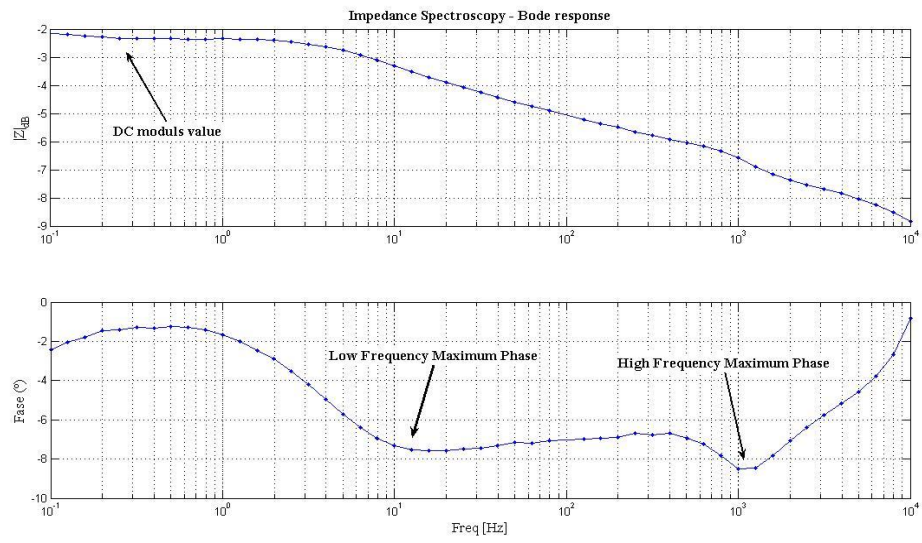


Fig. 8. EIS Relevant Characteristics b) Bode plot

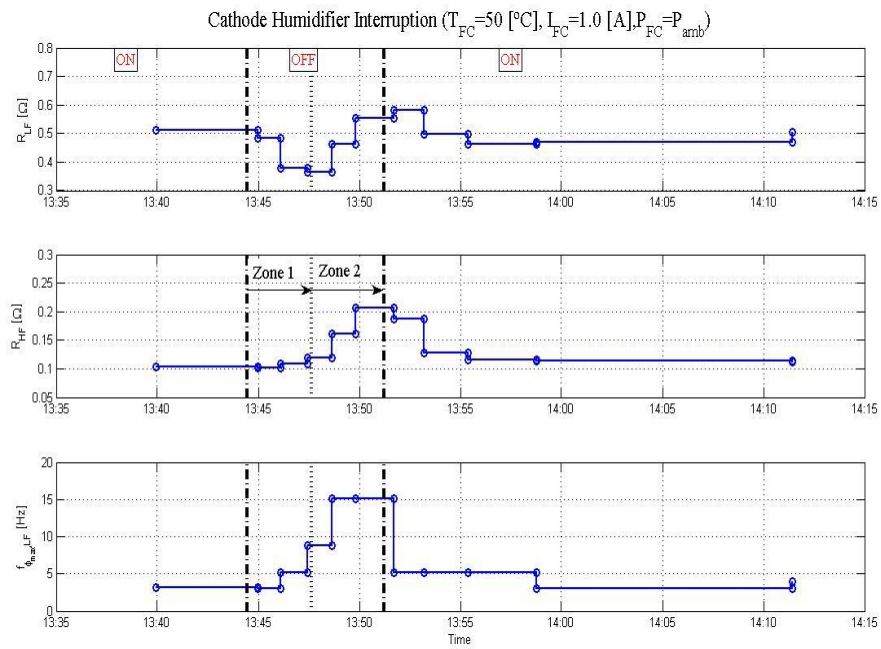


Fig. 9. Relevant Characteristics as performance indicators

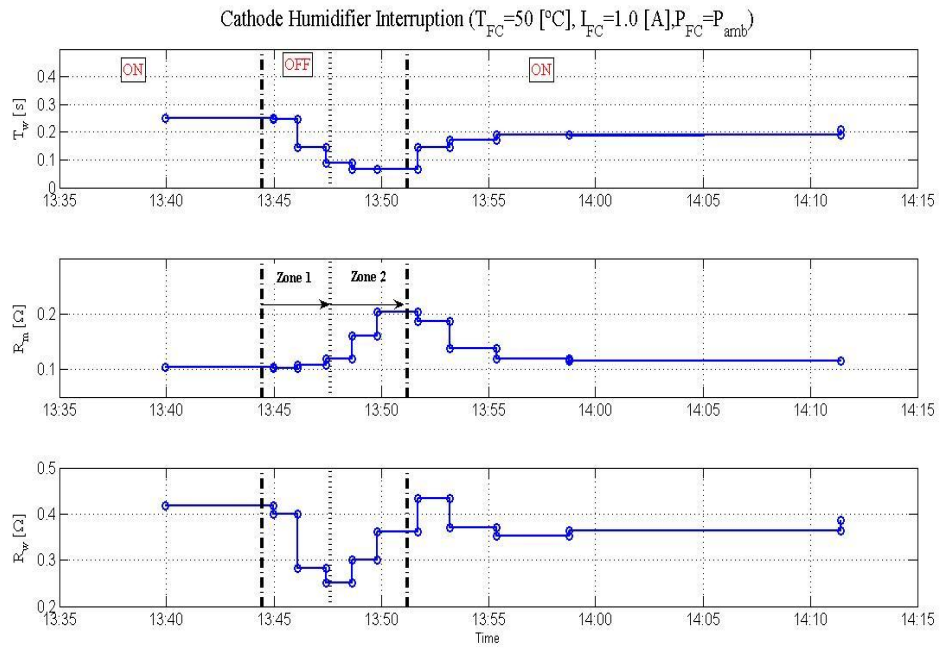


Fig. 10. Equivalent circuit parameters as performance indicators

JPS_Mauricio_Ve_captions.doc

[Click here to download Supplementary Materials: JPS_Mauricio_Ve_captions.doc](#)